





ORIGINAL ARTICLE

# Magnetic resonance imaging assessment of renal flow distribution patterns during ex vivo normothermic machine perfusion in porcine and human kidneys

ESOT 2021  
MILAN  
IN-PERSON & ONLINE

Rianne Schutter<sup>1</sup> , Veerle A. Lantinga<sup>1</sup>, Tim L. Hamelink<sup>1</sup>, Merel B. F. Pool<sup>1</sup> , Otis C. van Varsseveld<sup>1</sup>, Jan Hendrik Potze<sup>2</sup>, Jan-Luuk Hillebrands<sup>4</sup>, Marius C. van den Heuvel<sup>4</sup>, Rudi A. J. O. Dierckx<sup>2,3</sup>, Henri G. D. Leuvenink<sup>1</sup>, Cyril Moers<sup>1</sup> & Ronald J. H. Borra<sup>2,3</sup>

1 Department of Surgery – Organ Donation and Transplantation, University of Groningen, University Medical Center, Groningen, The Netherlands

2 Department of Radiology, University of Groningen, University Medical Center, Groningen, The Netherlands

3 Department of Nuclear Medicine, University of Groningen, University Medical Center, Groningen, The Netherlands

4 Department of Pathology & Medical Biology, University of Groningen, University Medical Center, Groningen, The Netherlands

## Correspondence

Rianne Schutter, Department of Surgery – Organ Donation and Transplantation, University Medical Center Groningen, Hanzeplein 1, Internal Postal Code BA42, 9713 GZ Groningen, The Netherlands.  
Tel./fax: +31 (0)6 3003 7096;  
e-mail: r.schutter@umcg.nl

## SUMMARY

Acceptance criteria of deceased donor organs have gradually been extended toward suboptimal quality, posing an urgent need for more objective pre-transplant organ assessment. Ex vivo normothermic machine perfusion (NMP) combined with magnetic resonance imaging (MRI) could assist clinicians in deciding whether a donor kidney is suitable for transplantation. Aim of this study was to characterize the regional distribution of perfusate flow during NMP, to better understand how ex vivo kidney assessment protocols should eventually be designed. Nine porcine and 4 human discarded kidneys underwent 3 h of NMP in an MRI-compatible perfusion setup. Arterial spin labeling scans were performed every 15 min, resulting in perfusion-weighted images that visualize intrarenal flow distribution. At the start of NMP, all kidneys were mainly centrally perfused and it took time for the outer cortex to reach its physiological dominant perfusion state. Calculated corticomedullary ratios based on the perfusion maps reached a physiological range comparable to in vivo observations, but only after 1 to 2 h after the start of NMP. Before that, the functionally important renal cortex appeared severely underperfused. Our findings suggest that early functional NMP quality assessment markers may not reflect actual physiology and should therefore be interpreted with caution.

*Transplant International* 2021; 34: 1643–1655

## Key words

arterial spin labeling, kidney, machine perfusion, magnetic resonance imaging, transplantation

Received: 25 June 2021; Revision requested: 13 July 2021; Accepted: 14 July 2021

## Introduction

### Organ quality assessment

The shortage of donor organs remains a persistent global problem. In order to bridge the gap between the supply of and the demand for donor organs, acceptance

criteria of deceased donor organs have been expanded, resulting in the increased use of suboptimal quality grafts. At present, 12–20% of procured deceased donor kidneys are discarded [1–4]. The main reason for kidneys to be declined for transplantation is presumed inferior organ quality. However, current clinical organ assessment strategies are predominantly subjective.

Inevitably, kidneys suitable for transplantation could incorrectly be discarded. Conversely, almost 25% of expanded criteria donor kidneys that were judged as acceptable for transplantation show a poor outcome after all [5]. Therefore, there is an urgent need for more objective and reliable pre-transplant donor organ assessment.

### Normothermic machine perfusion

Whereas hypothermic (1–7°C) machine perfusion (HMP) has been put into use as an improved donor kidney preservation method compared to static cooling [6], *ex vivo* normothermic machine perfusion (NMP) at temperatures around 35–37°C entails further advantages. Since cellular metabolism is reactivated in a near-physiological environment, NMP could assist clinicians in the decision of whether or not a donor kidney is suitable for transplantation. NMP has also been investigated as a renal preservation technique, as well as a platform for pre-transplant organ conditioning which might have the ability to mitigate ischemia–reperfusion injury [7–9]. In the UK, initially declined human kidneys, donated after circulatory death, were successfully transplanted after NMP assessment prior to transplantation [10]. In a porcine model, various durations of warm ischemia, perfusion characteristics, and perfusate biomarkers during NMP allowed to predict aspects of post-transplantation graft function to some extent [11].

Nevertheless, renal quality assessment during NMP remains in its infancy. In order to develop NMP as an organ quality assessment tool, there is a need to better understand the evolution of physiological conditions within the organ over time during perfusion, and how these differ from *in vivo* physiology. *Ex vivo* NMP assessment parameters that are currently considered are for example renal blood flow and macroscopic appearance of perfusion, but knowledge about the expected evolution of *ex vivo* regional perfusion distributions during NMP is currently lacking. Insight into such important intrarenal processes is essential to appreciate how measurements during NMP might convey reliable information about organ quality.

### Magnetic resonance imaging

Imaging techniques have the potential to provide a better understanding of intrarenal physiological processes and could elucidate unique information through imaging biomarkers of organ viability. While some techniques require the admission of exogenous contrast agents, non-contrast-enhanced techniques are preferable

since they avoid the risk of gadolinium-based nephrogenic systemic fibrosis [12]. Arterial spin labeling (ASL) is a functional magnetic resonance technique that uses water molecules as an endogenous contrast agent. ASL relies on magnetically tagging inflowing protons within a certain area of interest, (e.g., in the renal artery), and subsequently following these tagged protons while they move through a target volume such as a kidney. Over a defined period of time, “tagged” and “control” images are subtracted, resulting in a perfusion-weighted image in which signal intensity is proportional to perfusion. Since ASL does not require an exogenous contrast agent which could accumulate in the circulation and tissue, it is highly suited for serial monitoring of perfusion.

Our group has developed an MRI-compatible *ex vivo* NMP setup for human-sized kidneys to reliably perform warm perfusions for a prolonged period of time. The aim of this study was to characterize the regional distribution of renal blood flow during several hours of NMP, using ASL-derived perfusion maps as primary readout.

## Materials and methods

### Organ procurement

Nine viable porcine (female Dutch landrace pigs, around 130 kilograms) kidneys were procured from a local slaughterhouse, in accordance with all guidelines of the Dutch food safety authority. Twenty minutes after cardiac arrest of the pig, both kidneys were recovered en bloc. The kidney with the most favorable vasculature was connected to a pressure-controlled oxygenated HMP (1–5 °C) device (Kidney Assist Transport<sup>®</sup>, Xvivo, Göteborg, Sweden), primed with cold University of Wisconsin Machine Perfusion Solution (Belzer MPS<sup>®</sup>, Bridge to Life, Columbia, USA), at a pressure of 25 mmHg. Oxygenated HMP is the standard preservation method in The Netherlands for most kidneys donated after circulatory death and was used in our experiments to bridge the time interval between organ procurement and the availability of the MRI scanner, mimicking a clinically realistic cold organ preservation interval of approximately 10 hours. Oxygen was added to HMP, because of its proven beneficial effects in human and animal studies [13–19].

Four human discarded kidneys from deceased donors in the Netherlands were obtained after refusal by all transplant centers within the Eurotransplant region. We complied with our general infection prevention protocols when handling human and animal materials. Afterward, all surfaces were disinfected with 70% ethanol.

## Normothermic machine perfusion

Our MRI-compatible NMP perfusion setup (Fig. 1) consisted of a centrifugal pump (Medos Medizintechnik AG, Stolberg, Germany) controlled by custom-built hardware and custom-written software (LabView Software, National Instruments Netherlands B.V., Woerden, the Netherlands). The perfusate used for the porcine kidneys consisted of isolated autologous red blood cells (RBCs), crystalloids, albumin, creatinine, antibiotics, and electrolyte supplementation (Appendix 1). In the experiments with human discarded kidneys, washed human 0-negative RBCs from the blood bank were used, whereas all other perfusate additions remained the same. The perfusion solution was oxygenated and heated to 35–37°C by a clinical-grade oxygenator/heat exchanger (Hilite 800 LT, Medos Medizintechnik AG, Stolberg, Germany) supplied with carbogen (95% O<sub>2</sub>/5% CO<sub>2</sub>) at a rate of 0.5 ml/min. Renal flow rates were externally measured with an ultrasonic flow sensor (Transonic® HQXL Flowsensors, Ithaca, IL, USA). A SealRing® cannula (Organ Recovery Systems, Itasca, IL, USA) was placed around the aortic patch of the kidney, after which the kidney was positioned inside a custom-modified MRI-compatible organ chamber (LifePort®, Organ Recovery Systems, Itasca, IL, USA) in the isocenter of the MRI scanner, with 7.5m long polyvinylchloride tubing (inner diameter of 7mm) connecting the organ chamber to the other perfusion hardware that was located in the scanner's control room. Perfusion pressure was continuously measured in the arterial cannula, through 4 connected pressure lines measuring 2m each, with an inner diameter of 1.0mm (LectroCath V-Green PE, Vygon, Ecouen, France) hydraulically connected to a clinical-grade pressure sensor (TruWave disposable pressure transducer, Edwards Lifesciences, Irvine, CA, USA) positioned in the control room at the same height of the kidney.

## Perfusion protocol

We aimed to visualize intrarenal perfusion during the first 3 h of NMP with a constant pressure of 85 mmHg. ASL scans were performed every 15 min. After 3 h, in porcine kidneys, we also investigated the effect of hypotension on renal perfusion. Every 6 min, perfusion pressure was decreased in steps of 10 mmHg, from 85 mmHg to 25 mmHg, followed by a step-by-step increase back to 85 mmHg. After a short stabilization period of 3 min per step, ASL

scans were performed (Fig. 2). For logistical reasons, human discarded kidneys only underwent regular NMP for 3 h.

## Samples

Blood and urine samples were taken hourly and perfusate volume loss due to sampling was corrected with a similar volume of Sterofundin ISO (B. Braun Melsungen AG, Melsungen, Germany). Arterial blood gas samples were analyzed immediately, and results were used to guide electrolyte and glucose corrections. Venous samples were drawn from a 10Fr cannula (Nutrisafe Feeding Tube, Vygon, Ecouen, France) inside the renal vein, such that perfusate could still exit the vein without obstruction. Urine was collected through an 8Fr cannula (also Nutrisafe Feeding Tube) inserted in the ureter, and all urine not required for analyses was recirculated into the perfusion solution. Cortical punch biopsies (4 mm) were taken after HMP and at the end of NMP, paraffin-embedded and histologically evaluated by Periodic acid–Schiff (PAS) staining. Formulas used to estimate glomerular filtration rate, fractional sodium excretion, and oxygen consumption are available in the Appendix 1.

## MRI scan protocol

For all experiments, a clinical 3T Magnetom Prisma scanner (Siemens Healthineers, Erlangen, Germany) was used (software platform VE-11C). A 64-channel head-neck coil was positioned around the organ chamber with the kidney. The scanner's body coil was used as a transmit coil. ASL was performed using a standard 3D PASL product sequence-based acquisition in an oblique sagittal plane in order to scan roughly perpendicular to the renal artery. Each ASL acquisition employed a flow-sensitive alternating inversion recovery (FAIR-QII-) preparation with a three-dimensional gradient and spin echo (3D-GRASE) readout. The field of view was 188 × 188 mm, base resolution 64, resulting in a voxel size of 3 (slice thickness) × 2.94 × 2.94 mm (by means of interpolation 3 × 1.5 × 1.5 mm). For each scan, 28 slices were obtained, slice-oversampling was 20% and phase-oversampling 30%. Phase-encoding direction was antero-posterior. The repetition time was 5000 ms, echo time was 16.4 ms, and inversion time was 1990 ms. Bolus duration was set at 700 ms. The receiver bandwidth was 2604 Hz/pixel. Total acquisition time was 2:45 min. Fat saturation to suppress the signal of surrounding fat was applied.

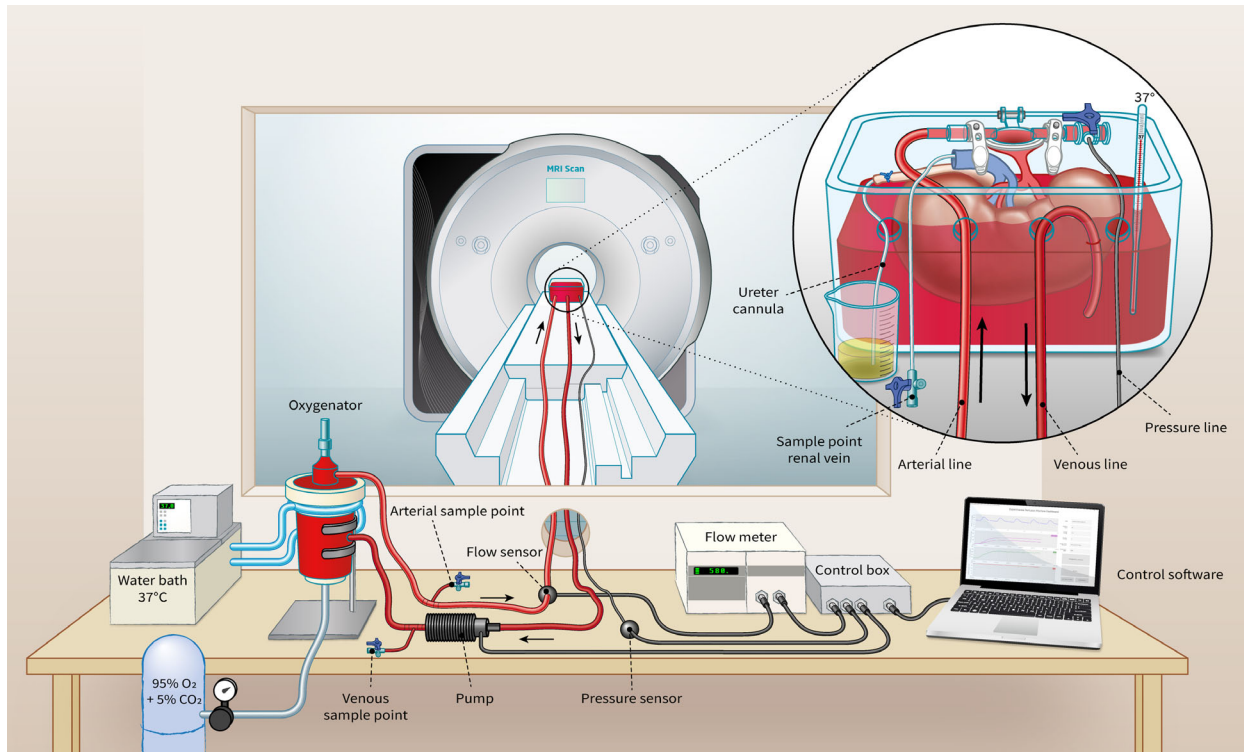


**Figure 1** MRI compatible setup for ex vivo normothermic human-sized kidney perfusion.

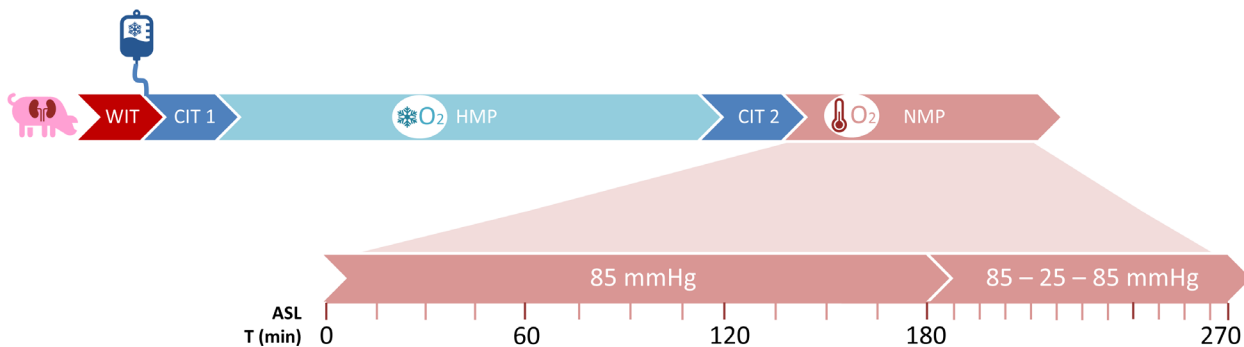


**Figure 2** Timeline depicting preservation and machine perfusion of each kidney. WIT: warm ischemia time, CIT1: cold ischemia time between the first cold flush and start of cold machine perfusion, HMP: hypothermic machine perfusion, CIT2: cold ischemia time between HMP and the start of NMP in which the kidney was prepared and cannulated on ice, NMP: normothermic machine perfusion, ASL: arterial spin labeling.

Once, a parallel simultaneous perfusion and scanning setup were performed with two human discarded kidneys with a peripheral angio 36 coil (Siemens Healthineers). Due to the adjusted position of these kidneys, acquisition of the ASL sequence was performed in a transversal plane. The field of view was  $320 \times 320$  mm; base resolution 64; resulting in a voxel size of  $3 \times 2.5 \times 2.5$  mm. Echo time was 15.82 ms. For each kidney, 60 slices were obtained. Other settings were similar to the single kidney scans with the 64-channel head-neck coil. Total duration of each scan was 5:25 min.

### Image analysis

ASL techniques are most suitable when data are processed in a relative sense, comparing corresponding regions within a single organ. Deriving absolute flow values would require multiple assumed or estimated parameters, which made us prefer a proportional, relative approach. Renal perfusion maps were visualized with Horos medical imaging/DICOM viewer (version 3.3.6, Horos Project) and resliced in the coronal plane for analysis. Regions of interest (ROI) were manually drawn on an overlay of a high-resolution

isotropic anatomical T2-weighted image and the corresponding ASL-derived perfusion map (Fig. 3). Cortical perfusion values were represented as the mean signal intensity of an ROI covering the outer renal cortex. To obtain a mean signal intensity of medullar perfusion, multiple ROIs were drawn into the medullary pyramids, identified on the anatomical T2-weighted image. Negative mean signal intensity of a single medullar ROI (resulting from the subtraction of the two primary ASL images) during a low state of perfusion was attributed to noise, in line with the deployed ASL approach being insensitive for very low perfusion rates. Mean signal intensity was then calculated with the remaining medullar ROIs.

### Statistics

All data are expressed as means  $\pm$  standard deviation. Statistical evaluation was performed with SPSS 23 (IBM, Armonk, New York, NY, USA). Mann–Whitney U tests were used to compare independent groups and Wilcoxon rank tests to compare repeated measurements when data were not normally distributed. All tests were 2-sided, and  $P$  values  $<0.05$  were considered to indicate statistical significance. GraphPad (version 8.4.2, GraphPad Prism, Miami, FL, USA) software was used to compose graphs.

## Results

### Intrarenal perfusion distribution

In all experiments, kidneys showed an evident visual perfusion shift over time toward the cortical area

(Fig. 4). At the start of NMP, only the central area of the kidney had a strong signal intensity, while it took at least 1–2 h before the outer cortex reached a dominant perfusion state. All kidneys appeared to have a macroscopically adequate perfusion, judging from a visually assessed homogeneously pink outer surface appearance already in the first minutes after the start of NMP. Hence, initial appearance of renal perfusion at visual inspection was very different from the perfusion distribution imaged with ASL.

Average total warm and cold ischemia times were comparable between porcine and human kidneys (Table 1), but given the last-minute nature of the procedures with discarded human kidneys, ischemia times could not be protocolized and were more diverse. Reasons for discard of the four human kidneys were as follows: one kidney was declined because malignant lymph nodes were discovered in the iliac area during procurement, one due to the organ's small overall size with multiple small cysts, and two kidneys from the same donor were rejected because of a positive donor hepatitis B virology test. After procurement, two human kidneys were statically stored on ice and two kidneys were preserved on a clinical HMP device. Human kidneys were smaller compared with porcine kidneys and mean externally measured flow (ml/min/100gr) was higher in the human kidney group. In the porcine group, CM ratios reached a plateau around 1.5–2 h of perfusion. In two human kidney experiments, a plateau comparable to the porcine group around 1.5 h was observed, whereas two other kidneys' CM ratios continued to increase after 3 h. No significant differences were observed between porcine and human CM ratios during 3 h of NMP.

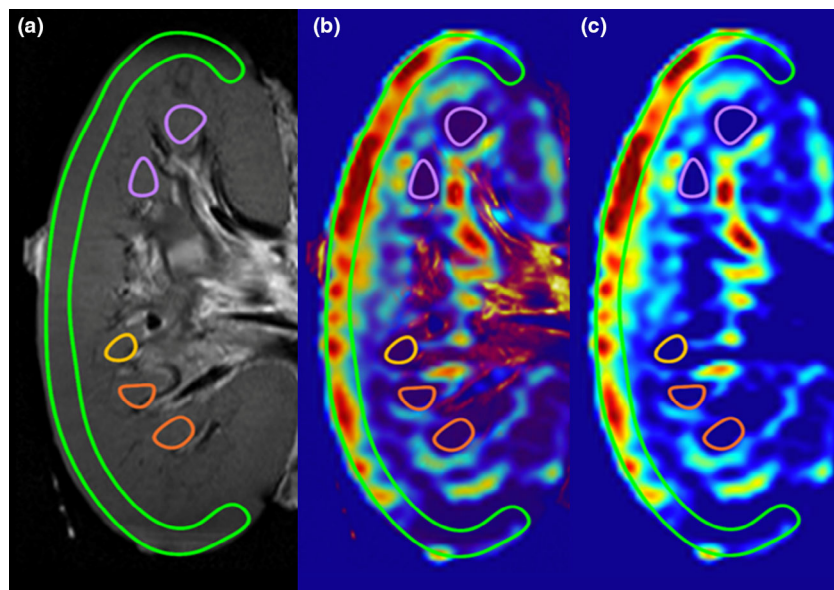


**Figure 3** Example of kidney segmentation for analysis of regional perfusion. (a) T2-weighted anatomical image in which the outer cortex and medullar pyramids were identified. (b) Overlay image of the T2-weighted image and ASL-derived perfusion map. (c) ASL-derived perfusion map with the identified ROIs.

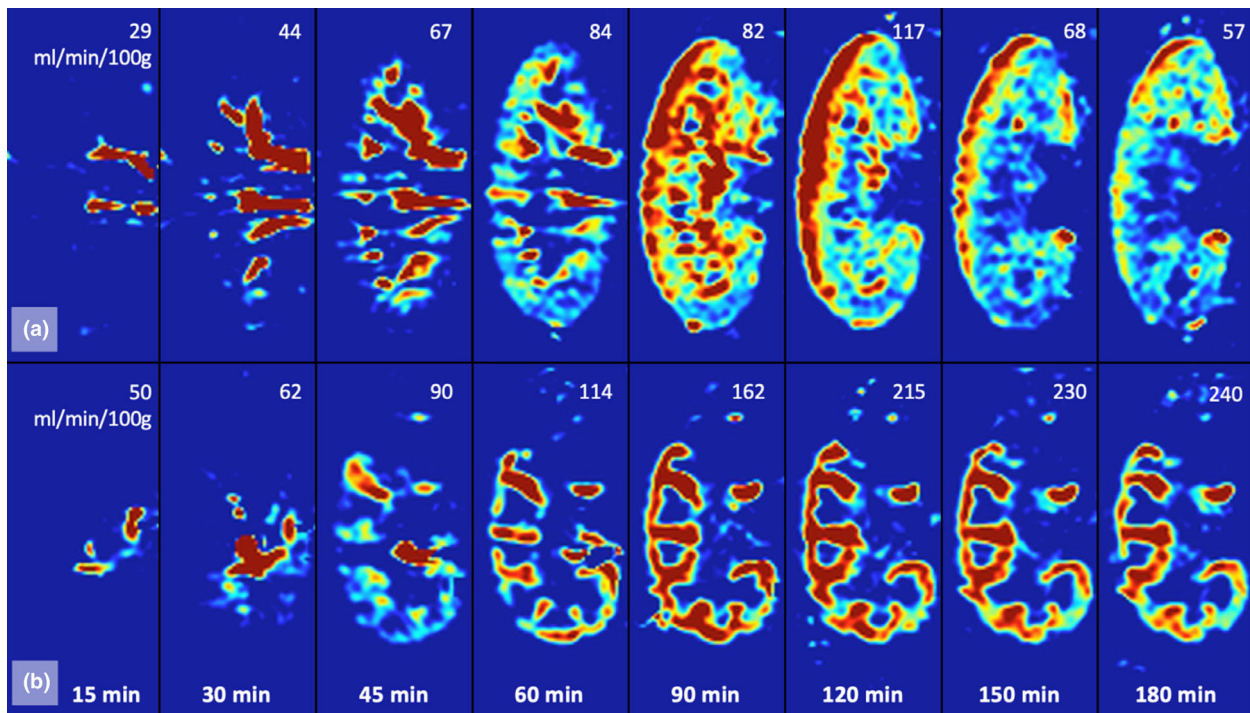


**Figure 4** ASL-derived coronally resliced perfusion map of a porcine (a) and a human (b) kidney over the first 180 minutes of normothermic machine perfusion. In the upper right corners are the corresponding renal perfusion rates in ml/min/100g.

**Table 1.** Baseline characteristics, externally measured total flow, and ASL perfusion-derived corticomedullary (CM) ratio of porcine and human discarded kidneys.

	Porcine kidney <i>n</i> = 9 Mean (SD)	Human kidney <i>n</i> = 4 Mean (SD)
Weight prior to NMP (g)	291 (±42)	224 (±69)
Warm ischemia time (min)	21 (±2)	22 (±13)
Total cold ischemia time (min)	695 (±19)	896 (±399)
Externally measured flow (ml/min/100g)		
30 min	83 (±39)	143 (±66)
60 min	117 (±31)	185 (±90)
120 min	129 (±51)	226 (±68)
180 min	116 (±46)	244 (±50)
ASL-derived perfusion signal intensity (CM ratio)		
30 min	2.1 (±2.1)	1.2 (±1.0)
60 min	5.0 (±5.0)	3.0 (±1.1)
120 min	6.5 (±6.4)	4.5 (±1.0)
180 min	5.3 (±3.7)	6.6 (±2.8)

The relation between the externally measured renal flow and CM ratio seemed very heterogeneous. In several cases, the kidney had a very stable total flow during the entire experiment, whereas the CM ratio displayed a completely different pattern with a clear increase over time. For example, one kidney had a constant flow of 74-

98ml/min/100g, while the CM ratio gradually rose from 0.45 to 6.10 (Fig. 5). These observations seem to indicate that externally measured renal flow does not give adequate insight into the intrarenal flow distributions and that entirely different regional flow distribution patterns exist over time within the same kidney with a stable flow.

Externally measured renal flow and corresponding ASL perfusion-derived CM ratios during the pressure step-down and step-up protocol after 3 h of NMP are presented in Table 2. It was notable that during the step-up phase, total renal flow did not recover to the equivalent values as seen at similar pressures during the preceding step-down phase. During hypoperfusion, CM ratios decreased rapidly, resulting in an intrarenal shift of perfusion from the cortical area to the medullar regions. In many cases, renal perfusion became ultimately too low to induce a measurable ASL signal. The total perfusate flow threshold for an adequate ASL signal within our particular setup was around 70 ml/min/100g.

#### Assessment of renal function over time

Since intrarenal flow distribution patterns changed over time, it seems likely that the different anatomical regions are served in an unequal pace from the start of NMP onwards. We hypothesized that this could also affect glomerular filtration rate (GFR), renal metabolism,

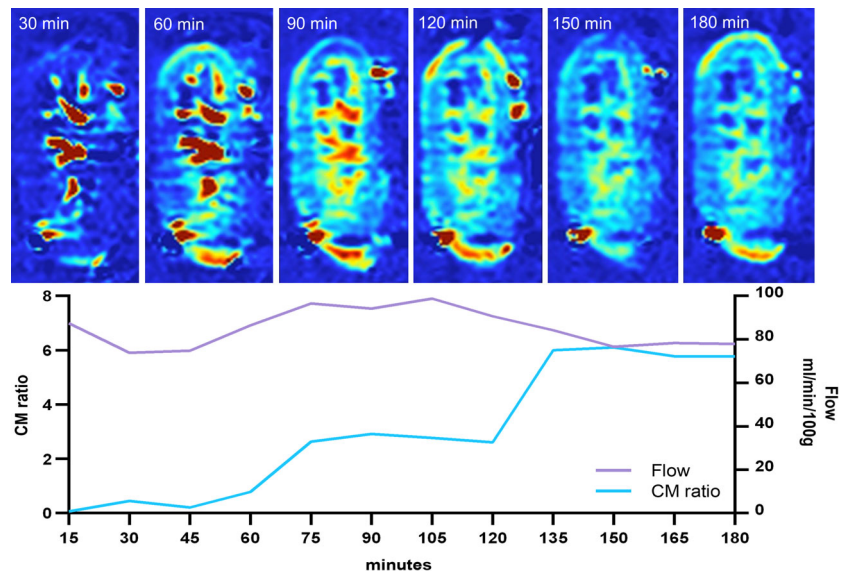


**Figure 5** Series of 1 porcine kidney with a continuous flow between 74–98 ml/min/100g and very diverse corresponding CM ratios.

**Table 2.** Decrease and increase of continuous arterial perfusion pressure from 85 mmHg to 25 mmHg and back in 9 porcine kidneys.

Continuous arterial pressure (mmHg)	Externally measured flow (ml/min/100g). Mean (SD)	CM ratio Mean (SD)
85 mmHg (baseline)	106 ( $\pm$ 38)	5.0 ( $\pm$ 4.1)
75 mmHg	95 ( $\pm$ 37)	5.1 ( $\pm$ 4.0)
65 mmHg	83 ( $\pm$ 34)	4.8 ( $\pm$ 3.6)
55 mmHg	69 ( $\pm$ 32)	3.7 ( $\pm$ 2.8)
45 mmHg	54 ( $\pm$ 29)	–*
35 mmHg	38 ( $\pm$ 25)	–*
25 mmHg (minimum)	24 ( $\pm$ 19)	–*
35 mmHg	37 ( $\pm$ 24)	–*
45 mmHg	48 ( $\pm$ 25)	1.7 ( $\pm$ 1.3) <sup>†</sup>
55 mmHg	58 ( $\pm$ 27)	2.2 ( $\pm$ 1.7) <sup>†</sup>
65 mmHg	68 ( $\pm$ 30)	2.9 ( $\pm$ 2.0) <sup>†</sup>
75 mmHg	78 ( $\pm$ 35)	3.1 ( $\pm$ 2.1)
85 mmHg	86 ( $\pm$ 34)	3.7 ( $\pm$ 3.4)

\*During severe hypoperfusion, most kidneys had no measurable ASL signal due to low perfusion. Therefore, no mean CM ratio was calculated.

<sup>†</sup>1 missing value.

cellular damage, and excretion function over time (Fig. 6). Within the porcine group, creatinine clearance, oxygen consumption, diuresis, and flow were relatively stable during the first 3 h of NMP and no significant differences were observed between the time points (1, 2, and 3 h) after the start of NMP. Fractional sodium excretion (FENa), however, was remarkably lower after 2 ( $P = 0.008$ ) and 3 h ( $P = 0.011$ ) compared with values

after 1 h of perfusion. The increase of injury marker ASAT per hour was significantly lower in the third NMP hour ( $P = 0.05$ ) compared with the second hour. LDH increase in the perfusate also diminished per hour, with a significant difference between the first and third hour ( $P = 0.008$ ). The human kidney group had a distorted baseline perfusate content with much higher lactate, ASAT, and LDH, probably due to higher hemolysis of human banked erythrocytes, compared with freshly fractionated autologous porcine red cells. Initial lower pH needed to be corrected with additional sodium bicarbonate, resulting in higher overall sodium levels. Within this small and heterogeneous human kidney group, no statistical differences could be found between the time points.

### Histology

Porcine kidney biopsies taken prior to NMP showed acute tubular necrosis (ATN), with loss of brush border, flattened epithelia, epithelial vacuolization, and apoptosis. This damage was almost solely visible in proximal tubuli. Distal tubuli and glomeruli had a normal appearance. Histological analysis of human discarded kidneys revealed presence of some pre-existent damage with interstitial fibrosis, glomerular damage, and tubular atrophy. Biopsies taken at the end of NMP in both groups showed worsening of ATN when compared to pre-NMP biopsies and more edema (Fig. 7).

### Discussion

This pilot study is the first to visualize the regional distribution of renal perfusate flow with magnetic

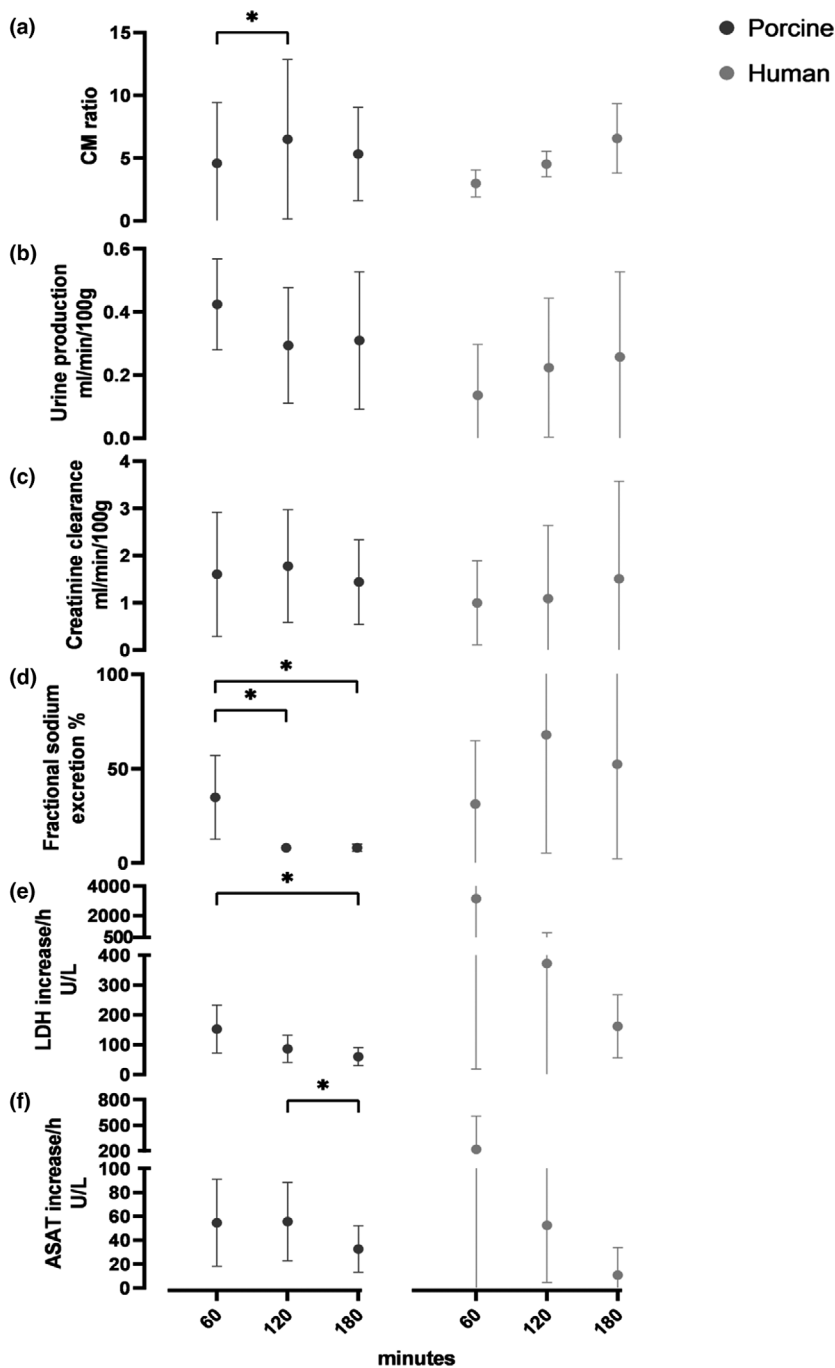


**Figure 6** Renal quality assessment markers of 9 porcine and 4 human discarded kidneys during NMP. Mean (SD). (a) mean corticomedullary ratio from the ASL-derived perfusion map. (b) urine production per hour. (c) creatinine clearance per hour. (d) fractional sodium excretion per hour. (e) hourly increase of lactate dehydrogenase (LDH). (f) hourly increase of aspartate aminotransferase (ASAT).

resonance techniques during the first hours of *warm* ex vivo perfusion in porcine and human kidneys. Previous in vivo studies employing ASL-based perfusion imaging showed CM ratios between 3.1 and 7.2 in healthy volunteers [20–24]. *In our experiments, these in vivo physiological ranges were met only after 1-2 hours of NMP.* It seems fair to question whether kidneys from relatively young animals would show the same intrarenal distribution compared with human discarded kidneys from older suboptimal donors. Nevertheless, the similarities

over time that we found for both types of kidneys have encouraged us to continue using porcine kidneys as a suitable model to obtain a better understanding of basic physiological responses during warm perfusion.

Current literature suggests that blood entering the kidney via the renal artery is distributed via the large interlobar arteries, branching into arcuate arteries and further into smaller interlobular arteries, which ascend through the cortex and form the origin of afferent arterioles. After the glomerular capillary tufts, only 10% of



the blood flow perfuses the renal medulla via the efferent arterioles that cross the corticomedullar border and give rise to the vasa recta in the outer medulla [25,26]. According to this “serial” vascular anatomy, all medullar blood must originate from the cortical post-glomerular vasculature. In our calculation of the CM ratio, medullar ROIs were drawn into the medullar pyramids, avoiding artifacts of the central larger vessels. A low CM ratio implies a relatively high perfusate flow through the medulla, despite a low flow through the cortical area. This finding challenges the aforementioned “serial” vasculature dogma, suggesting that some kind of shunting takes place through vascular pathways that might be too small to visualize. Another explanation could be the role of the inner cortex (near and in between the pyramids) that is left out of our CM ratio calculation, but might be able to forward cortical perfusion to the central area via juxtglomerular nephrons. Nevertheless, an increase in CM ratio over time marks a delayed reperfusion of the important outer cortex containing the cortical nephrons that account for 70–80% of all nephrons [27].

Alterations in cortical and medullar blood flow after ischemia–reperfusion injury (IRI) have been studied in several animal models. Regner *et al.* concluded that cortical blood flow (CBF) fully recovers after 30–45 minutes of IRI, while outer medullar blood flow (MBF) is associated with a prolonged secondary drop in blood flow [28]. Our experimental kidneys were exposed to much longer ischemia times, but the cortical signal intensity on the perfusion maps gradually increased over time, whereas the mean medullar signal intensity had an average decreasing trend. Increasing CM ratios could therefore also be explained by the theory that MBF might be impaired. In vivo CBF is well known to be autoregulated, but MBF regulation remains controversial and poorly understood [25,29]. The integrity and importance of the ex vivo renal cortical autoregulation after episodes of warm and cold ischemia remain unclear, warranting further study.

With an increasing number of transplant centers adopting clinical NMP technology, a better understanding of renal physiology during the course of warm perfusion is necessary to develop reliable quality assessment tools. Hosgood *et al.* developed a viability score after 60 min of NMP based on the kidney’s macroscopic appearance, renal perfusate flow, and urine production of procured human kidneys that were deemed unsuitable for transplantation, after which kidneys with a presumably favorable score were successfully transplanted [10,30]. However, due to varying approaches and protocols regarding NMP assessment prior to transplantation by different research groups, there is no consensus yet

on important issues such as the duration of NMP, perfusate composition, optimal hemodynamic conditions, or reliable viability markers [31].

We found that fractional sodium excretion was significantly lower after 2 and 3 h of NMP compared with the first hour. The high initial excretion of sodium might be caused by the lack of passive reabsorption in the damaged proximal tubuli. As time passes during NMP, it might be possible that sodium–potassium ATPase pumps in the thick ascending limb of Henle’s loop become activated and foster sodium reabsorption. Under normal physiological conditions, the kidney only extracts 10–15% of oxygen from the arterial blood [32]. Yet 80% of the renal oxygen consumption is used to power tubular sodium reabsorption [33]. Oxygen consumption in our experiments was very heterogenous between the different time points. This might be explained by differences in the rate at which each individual kidney warmed up, the possible generation of reactive oxygen species by mitochondria due to ischemia–reperfusion injury [34], or the varying influence of arterial–venous oxygen shunting [35]. Additional functional MRI techniques that visualize oxygen availability could provide essential supplemental information to better understand ex vivo renal oxidative metabolism [36].

Renal perfusion imaging techniques have significant limitations, because of the absence of a practical gold-standard technique. However, renal perfusion measured by ASL-derived perfusion metrics has been previously validated against reference in vivo methods and showed good reproducibility in general, with overall poorer performance in the medulla than the renal cortex [37]. The main challenge is the relatively intrinsic poor signal-to-noise ratio (SNR), compared with contrast-enhanced methods. Only inflowing protons (present in water contained in the blood or perfusate) are marked as a tracer, which is just a small proportion of the total amount of water within the kidney tissue. Hence, regions with a physiologically lower perfusion such as the renal medulla suffer more from this limitation. To mitigate this, multiple label and control pairs were acquired and subsequently averaged to increase SNR. In our experiments, we experienced severe signal loss when the kidney had a total renal perfusion of less than 70ml/100gr/min and, therefore, these data are less reliable.

Important ASL acquisition parameters are the labeling period (determining bolus size) and the post labeling delay (PLD) between labeling and imaging (allowing the bolus to reach the target tissue). In our experiments renal flow had serious fluctuations, especially within the first hour of NMP. We used fixed bolus duration times, independent from the actual renal flow at that time,

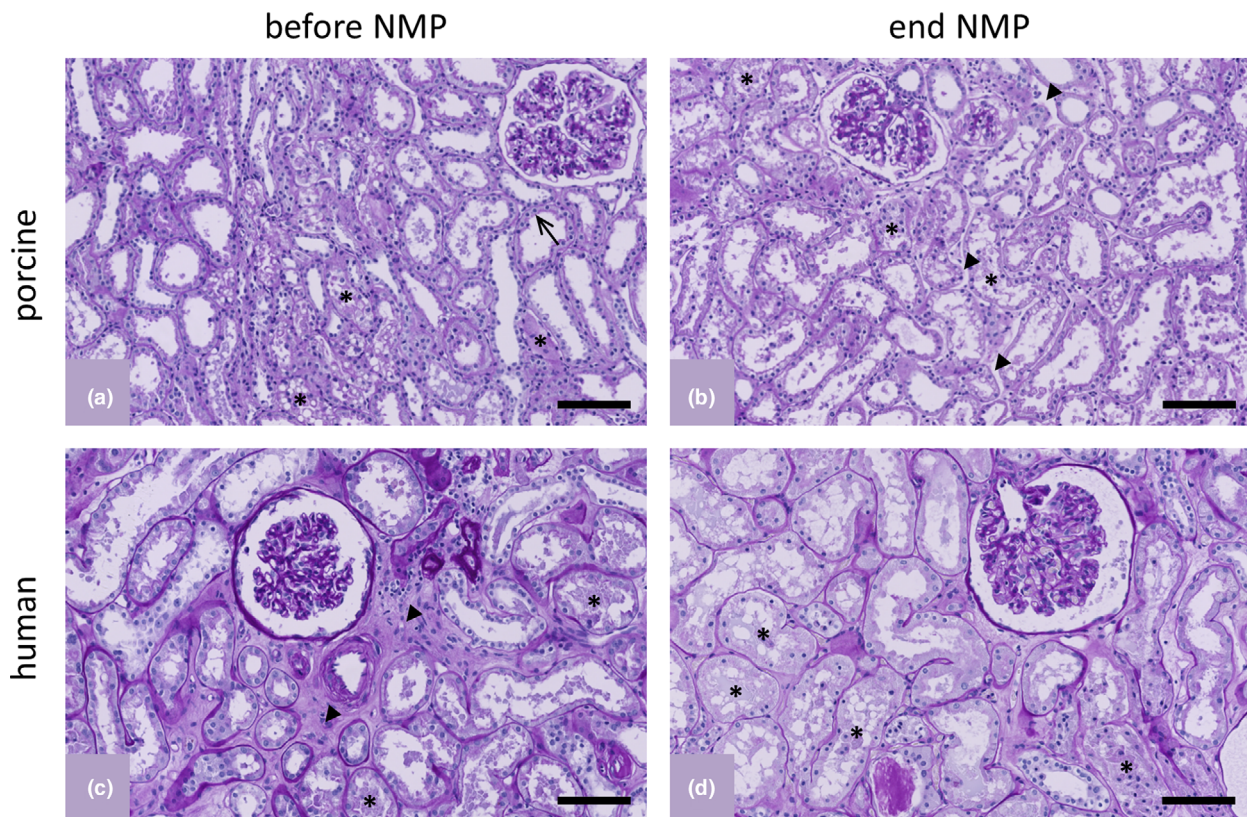


**Figure 7** Histology (20x magnification) of biopsies taken just before start of NMP and at the end of NMP. (a) porcine kidney before NMP, showing ATN. As an example three proximal tubuli with ATN are marked with asterisks, the arrow indicates a representative healthy proximal tubule with PAS-positive brush border. (b) same porcine kidney after NMP, with increased edema (arrowheads) and ATN (asterisks). (c) discarded human kidney from a 71-year-old DBD donor with a suspected malignancy (outside the kidney) before NMP, with pre-existent interstitial fibrosis (arrowheads) and mild ATN (asterisks) in the proximal tubuli. (d) same human kidney after NMP, showing signs of increased ATN (asterisks). Scale bar: 100  $\mu$ m.

sometimes resulting in a suboptimal labeling period and delay. If the PLD is too short, the measured perfusate flow will be underestimated, and the residual labeled spins appear as an intra-arterial transit artifact. If the PLD is too long (or total renal flow relatively high), the labeled bolus does not reach the target renal tissue, but the extra time causes decay of the label, resulting in a reduced signal. Future experiments will be performed with more flow-customized acquisition strategies.

Disadvantages of MRI are the relatively high costs and complicated logistics, especially when combined with NMP in a tethered setup such as our current one. But these limitations are inherent to development of most new techniques that are still in their infancy. Because of logistic reasons, we were limited to an NMP duration of 3 h NMP in the present study. However, our research group has further optimized logistics and is currently performing similar experiments in a porcine model with an NMP duration of 6 h. In addition, our group is currently developing an MRI-compatible portable warm perfusion machine, which could greatly simplify swift pre-

transplant MRI assessment of donor kidneys. The remaining logistical efforts as well as costs could become acceptable if the method proves to provide sufficient diagnostic value in clinical practice, potentially leading to more available donor kidneys when organs that are currently discarded can be reliably evaluated *ex vivo* and some deemed suitable for transplant after all.

While other radiologic modalities such as Doppler ultrasound and computed tomography can provide insight into renal anatomy, vasculature, tissue echogenicity, and perfusion velocity, functional MRI can convey much more information about organ quality in terms of physiology and metabolism. ASL, for example, provides information about actual regional flow (i.e., volume per unit of time, not just perfusion velocity in terms of distance per unit of time which Doppler ultrasound can quantify). It is perfusate flow and not perfusion velocity which eventually determines the absolute supply of oxygen and nutrients to the renal tissue and being able to quantify flow allows to estimate the extent to which these important determinants of healthy renal metabolism are

within an acceptable range. In our present study, we chose to focus on ASL as a measure of regional perfusion of renal grafts, but there are many other very promising functional MRI acquisition techniques, such as quantifying intrarenal regional oxygen delivery and consumption with blood oxygen level dependent (BOLD), measuring the slope of renal metabolite synthesis with MR spectroscopy and detection of the amount of graft fibrosis through diffusion tensor imaging and MR elastography [38]. Given this huge potential, we feel that ex vivo functional MRI could provide valuable pre-transplant imaging biomarkers that evaluate important aspects of renal pathology, physiology, and metabolism to a much greater extent than more conventional techniques such as ultrasound can do.

### Conclusion

This study found that intrarenal flow distribution changes after the start of *warm* ex vivo perfusion and it takes 1 to 2 h before an adequate, in vivo like cortical perfusion is achieved. Since the majority of nephrons are located in the renal cortex, renal function may not recover at the same rate as total renal blood flow does during NMP. Quality assessment markers measured early after the start of NMP should therefore be interpreted cautiously. Given the rapidly increasing popularity of renal NMP, our study suggests that imaging can help to better characterize ex vivo kidney physiology and stresses the importance of studies which unravel ex vivo renal autoregulation and metabolism in order to develop relevant quality assessment strategies.

### Authorship

R. Schutter and A. Lantinga involved in design research, acquisition, analysis, interpretation, and writing manuscript. T.L. Hamelink, M.B.F. Pool, and O.C. van

Varsseveld involved in acquisition. J.H. Potze, J.L. Hillebrands, and M. van den Heuvel involved in acquisition and analysis. R.A.J.O. Dierckx involved in critical revision. H.G.D. Leuvenink performed design research and critical revision. C. Moers involved in design research, acquisition, interpretation, and critical revision. R.J.H. Borra involved in design research, acquisition, analysis, interpretation, and critical revision.

### Funding

This research was supported by the Dutch Kidney Foundation and the European Research Council.

### Conflict of interest

All authors declare no conflict of interest.

### Acknowledgements

Ir. P.J. Ottens involved in analysis of perfusate and urine samples.

### Ethical approval

According to Dutch law, permission from an ethics review committee is not required when a study involves human subjects who have passed away. The Dutch law on organ donation rules that people who give permission for organ donation, automatically also provide consent for transplantation-related research with their organs if an organ is discarded, unless the person explicitly objected. Therefore, it is (by law) not even required to ask consent from their relatives. For ethical reasons, however, we did ask permission, and in every case, written consent was obtained from the donor family.

## REFERENCES

1. Eurotransplant annual reports. Available online: <https://www.eurotransplant.org/statistics/annual-report>. Accessed on 1 May 2020.
2. NHS. The National Organ Retrieval Service and Usage of Organs 2018-2019. Available online: <https://www.organdonation.nhs.uk/helping-you-to-decide/about-organ-donation/statistics-about-organ-donation/transplant-activity-report/>. Assessed on 11 May 2020.
3. Stewart DE, Garcia VC, Rosendale JD, Klassen DK, Carrico BJ. Diagnosing the decades-long rise in the deceased donor kidney discard rate in the United States. *Transplantation* 2017; **101**: 575.
4. Callaghan CJ, Harper SJ, Saeb-Parsy K, et al. The discard of deceased donor kidneys in the UK. *Clin Transplant* 2014; **28**: 345.
5. Schnitzler MA, Lentine KL, Gheorghian A, Axelrod D, Trivedi D, L'Italien G. Renal function following living, standard criteria deceased and expanded criteria deceased donor kidney transplantation: impact on graft failure and death. *Transpl Int* 2012; **25**: 179.
6. Moers C, Smits JM, Maathuis MH, et al. Machine perfusion or cold storage in deceased-donor kidney transplantation. *N Engl J Med* 2009; **360**: 7.
7. Chandak P, Phillips BL, Uwechue R, et al. Dissemination of a novel organ

- perfusion technique: ex vivo normothermic perfusion of deceased donor kidneys. *Artif Organs* 2019; **43**: E308–E319.
8. Hosgood SA, Saeb-Parsy K, Wilson C, Callaghan C, Collett D, Nicholson ML. Protocol of a randomised controlled, open-label trial of ex vivo normothermic perfusion versus static cold storage in donation after circulatory death renal transplantation. *BMJ Open* 2017; **7**: e012237.
  9. DiRito JR, Hosgood SA, Tietjen GT, Nicholson ML. The future of marginal kidney repair in the context of normothermic machine perfusion. *Am J Transplant* 2018; **18**: 2400.
  10. Hosgood SA, Thompson E, Moore T, Wilson CH, Nicholson ML. Normothermic machine perfusion for the assessment and transplantation of declined human kidneys from donation after circulatory death donors. *Br J Surg* 2018; **105**: 388.
  11. Kathis JM, Hamar M, Echeverri J, et al. Normothermic ex vivo kidney perfusion for graft quality assessment prior to transplantation. *Am J Transplant* 2018; **18**: 580.
  12. Schieda N, Blaichman JJ, Costa AF, et al. Gadolinium-based contrast agents in kidney disease: A comprehensive review and clinical practice guideline issued by the canadian association of radiologists. *Can J Kidney Health Dis* 2018; **5**: 2054358118778573.
  13. Jochmans I, Brat A, Davies L, et al. Oxygenated versus standard cold perfusion preservation in kidney transplantation (COMPARE): a randomised, double-blind, paired, phase 3 trial. *Lancet* 2020; **396**: 1653.
  14. Patel K, Smith TB, Neil DAH, et al. The effects of oxygenation on ex vivo kidneys undergoing hypothermic machine perfusion. *Transplantation* 2019; **103**: 314.
  15. Darius T, Gianello P, Vergauwen M, et al. The effect on early renal function of various dynamic preservation strategies in a preclinical pig ischemia-reperfusion autotransplant model. *Am J Transplant* 2019; **19**: 752.
  16. Venema LH, Brat A, Moers C, et al. Effects of oxygen during long-term hypothermic machine perfusion in a porcine model of kidney donation after circulatory death. *Transplantation* 2019; **103**: 2057.
  17. Thuillier R, Allain G, Celhay O, et al. Benefits of active oxygenation during hypothermic machine perfusion of kidneys in a preclinical model of deceased after cardiac death donors. *J Surg Res* 2013; **184**: 1174.
  18. Buchs JB, Lazeyras F, Ruttimann R, Nastasi A, Morel P. Oxygenated hypothermic pulsatile perfusion versus cold static storage for kidneys from non heart-beating donors tested by in-line ATP resynthesis to establish a strategy of preservation. *Perfusion* 2011; **26**: 159.
  19. Treckmann J, Nagelschmidt M, Minor T, Saner F, Saad S, Paul A. Function and quality of kidneys after cold storage, machine perfusion, or retrograde oxygen persufflation: results from a porcine autotransplantation model. *Cryobiology* 2009; **59**: 19.
  20. Artz NS, Sadowski EA, Wentland AL, et al. Arterial spin labeling MRI for assessment of perfusion in native and transplanted kidneys. *Magn Reson Imaging* 2011; **29**: 74.
  21. Haddock B, Larsson HBW, Francis S, Andersen UB. Human renal response to furosemide: Simultaneous oxygenation and perfusion measurements in cortex and medulla. *Acta Physiol (Oxf)* 2019; **227**: e13292.
  22. Wang J, Zhang Y, Yang X, et al. Hemodynamic effects of furosemide on renal perfusion as evaluated by ASL-MRI. *Acad Radiol.* 2012; **19**: 1194.
  23. Gardener AG, Francis ST. Multislice perfusion of the kidneys using parallel imaging: image acquisition and analysis strategies. *Magn Reson Med* 2010; **63**: 1627.
  24. Fenchel M, Martirosian P, Langanke J, et al. Perfusion MR imaging with FAIR true FISP spin labeling in patients with and without renal artery stenosis: initial experience. *Radiology* 2006; **238**: 1013.
  25. Pallone TL, Silldorff EP, Turner MR. Intrarenal blood flow: microvascular anatomy and the regulation of medullary perfusion. *Clin Exp Pharmacol Physiol* 1998; **25**: 383.
  26. Thomas L, Pallone AE, Mattson DL. Comprehensive physiology. 2012.
  27. A.C. Guyton JEH. Medical Physiology. Unit V. The kidney and body fluids. Tenth edition. ed2000.
  28. Regner KR, Roman RJ. Role of medullary blood flow in the pathogenesis of renal ischemia-reperfusion injury. *Curr Opin Nephrol Hypertens* 2012; **21**: 33.
  29. Pallone TL, Zhang Z, Rhinehart K. Physiology of the renal medullary microcirculation. *Am J Physiol Renal Physiol* 2003; **284**: F253–F266.
  30. Hosgood SA, Barlow AD, Dormer J, Nicholson ML. The use of ex-vivo normothermic perfusion for the resuscitation and assessment of human kidneys discarded because of inadequate in situ perfusion. *J Transl Med* 2015; **13**: 329.
  31. Elliott TR, Nicholson ML, Hosgood SA. Normothermic kidney perfusion: An overview of protocols and strategies. *Am J Transplant* 2021; **21**: 1382.
  32. Levy MN. Effect of variations of blood flow on renal oxygen extraction. *Am J Physiol* 1960; **199**: 13.
  33. Evans RG, Ince C, Joles JA, et al. Haemodynamic influences on kidney oxygenation: clinical implications of integrative physiology. *Clin Exp Pharmacol Physiol* 2013; **40**: 106.
  34. Kalogeris T, Bao Y, Korhuis RJ. Mitochondrial reactive oxygen species: a double edged sword in ischemia/reperfusion vs preconditioning. *Redox Biol* 2014; **2**: 702.
  35. Kuo W, Kurtcuoglu V. Renal arteriovenous oxygen shunting. *Curr Opin Nephrol Hypertens* 2017; **26**: 290.
  36. Pruijm M, Mendichovszky IA, Liss P, et al. Renal blood oxygenation level-dependent magnetic resonance imaging to measure renal tissue oxygenation: a statement paper and systematic review. *Nephrol Dial Transplant* 2018; **33** (suppl\_2): ii22–ii28.
  37. Odudu A, Nery F, Hartevelde AA, et al. Arterial spin labelling MRI to measure renal perfusion: a systematic review and statement paper. *Nephrol Dial Transplant* 2018; **33**(suppl\_2): ii15–ii21.
  38. Zhou JY, Wang YC, Zeng CH, Ju SH. Renal functional MRI and Its application. *J Magn Reson Imaging* 2018; **48**: 863.

## APPENDIX 1

## Perfusate composition

Autologous red blood cells*	544 ml
Sodium chloride 0.9% (Fresenius Kabi Nederland B.V., Zeist, Netherlands)	600 ml
Glucose 5% (Baxter BV, Utrecht, Netherlands)	20 ml
Human albumin 20% (Albuman 200 g/l, Sanquin Plasma Products B. V., Amsterdam, Netherlands)	200 ml
Sodium bicarbonate 8.4% (B. Braun Melsungen AG, Melsungen, Germany)	16 ml
Calcium gluconate 10% (B. Braun )	10 ml
Amoxicillin/clavulanic acid (Sandoz B.V., Almere, Netherlands)	1200 mg (in 20ml water solution)
Mannitol (Baxter B.V.)	32 mg
Creatinine (Sigma-Aldrich, Zwijndrecht, Netherlands)	160 mg
Insulin (Novo Nordisk A/S, Bagsværd, Denmark)	16 U
Sterofundin ISO (B. Braun)	Added 20 ml every hour
Amoxicillin/clavulanic acid	Added 192 mg (3.2 ml) every hour
Calcium gluconate 10%	Added 3 ml if calcium <1.1 mmol/l
Glucose 5%	Added 13 ml if glucose <4.6 mmol/l

\*Autologous blood from each pig was obtained and mixed with 25,000 units of heparin (LEO<sup>®</sup> pharma, Ballerup, Denmark). Whole blood was depleted of leukocytes using a leukocyte filter (BioR 02 plus BS PF, Fresenius Kabi, Zeist, the Netherlands) after which a red blood cells (RBC) concentrate was obtained by centrifuging, removing supernatant plasma, washing with phosphate-buffered saline, centrifuging again, and separating the pure RBCs.

## Additional formulas from methods and materials

$$\text{Glomerular filtration rate} \left[ \frac{\text{ml}}{\text{min}} \right] = \frac{\text{diuresis} * \text{Creat}_{\text{urine}}}{\text{Creat}_{\text{plasma}}}$$

Diuresis in ml/min/100gr and creatinine concentration in mmol/l

$$\text{Fractional sodium excretion} [\%] = \frac{\text{Na}_{\text{urine}} * \text{Creat}_{\text{plasma}}}{\text{Na}_{\text{plasma}} * \text{Creat}_{\text{urine}}} * 100$$

Sodium (Na) concentration and creatinine concentration in mmol/l

$$\text{Oxygen consumption} \left[ \frac{\text{ml}}{\text{min}} \right] = \frac{\text{Hb} * 0.024794 * (100 - sO_{2\text{venous}}) + K * (pO_{2\text{arterial}} - pO_{2\text{venous}})}{g} \times Q \times 100$$

Hemoglobin (Hb) is the perfusates Hb in mmol/l, pO<sub>2</sub> is the partial oxygen pressure arterial or venous in kPa, K is the solubility constant of oxygen in water at 37°C and equals 0.0225 (mL O<sub>2</sub> per kPa), sO<sub>2</sub> is the saturation in %, Q is the renal blood flow in dL/min, and g is the kidney weight in grams.